View metadata, citation and similar papers at core.ac.uk
brought to you by CORE
provided by Servicio de Coordinación de Bibliotecas de la Universidad Politécnica de Madrid

IN-SITU AND EX-SITU CHARACTERIZATION OF III-V SEMICONDUCTOR MATERIALS AND SOLAR CELLS UPON 10 MEV PROTON IRRADIATION

E. Yaccuzzi[1,2], E. Barrigón[3], S. Rodriguez[1], M. Ochoa[3], M. Barrera[1,2], P.Espinet-González[3], J. Garcia[1,2], M.L. Ibarra[1,2], H. Socolovsky[1], M.D. Perez[1,2], P. Giudici[1,2], M. Alurralde[1], C. Algora[3], I. Rey-Stolle[3], J. Plá[1,2]
[1]Departamento Energía Solar - Gerencia Investigación y Aplicaciones - CNEA, Argentina
[2]Consejo Nacional de Investigaciones Científicas y Técnicas (CONICET), Argentina
Av. General Paz 1499 - (1650) San Martín – Argentina
Tel. (+54-11) 6772-7128, Fax (+54-11) 6772-7121, jpla@tandar.cnea.gov.ar
[3]Instituto de Energía Solar – Universidad Politécnica de Madrid, Spain
Av.. Complutense 30; 28040 Madrid -Spain

ABSTRACT: In this work we present the results and analysis of a 10 MeV proton irradiation experiment performed on III-V semiconductor materials and solar cells. A set of representative devices including lattice-matched InGaP/GaInAs/Ge triple junction solar cells and single junction GaAs and InGaP component solar cells and a Ge diode were irradiated for different doses. The devices were studied in-situ before and after each exposure at dark and 1 sun AM0 illumination conditions, using a solar simulator connected to the irradiation chamber through a borosilicate glass window. Ex-situ characterization techniques included dark and 1 sun AM0 illumination I-V measurements. Furthermore, numerical simulation of the devices using D-AMPS-1D code together with calculations based on the TRIM software were performed in order to gain physical insight on the experimental results. The experiment also included the proton irradiation of an unprocessed Ge solar cell structure as well as the irradiation of a bare Ge(100) substrate. Ex-situ material characterization, after radioactive deactivation of the samples, includes Raman spectroscopy and spectral reflectivity.
Keywords: Radiation Damage, III-V Semiconductors, Multijunction Solar Cell

1 INTRODUCTION

The Solar Energy Department (DES) of the Argentine Atomic Energy Commission (CNEA) and the Institute of Solar Energy (IES) of the Polytechnic University of Madrid (UPM), collaborate in a scientific project devoted to the study of III-V semiconductor-based solar cells. Both groups have complementary experiences: the DES is mainly focused on simulation, testing and characterization of III-V devices for space applications, while the IES performs fabrication, testing, simulation and characterization of solar cells for terrestrial concentrating photovoltaics (CPV). In the frame of the mentioned collaboration, we performed an irradiation experiment at CNEA using 10 MeV protons generated by the electrostatic tandem accelerator TANDAR. The irradiated samples include InGaP, GaAs, triple junction (3JSC) InGaP/Ga(In)As/Ge solar cells, a Ge diode and GaAs/InGaP/Ge (Ge cell structure), fabricated at IES, as well as unprocessed Ge wafers.

The experiment included fluence calculation, in-situ dark and illuminated I-V curve measurements and numerical modeling. Ex-situ measurements were also performed, including Raman spectroscopy and spectral reflectivity characterization on the material samples.

Several results are presented: the damage estimation through PKAs (primary knock-on atoms) simulations for all tested devices (section 2), the evaluation of dark and illuminated in-situ I-V measurements (section 3), the device simulation applied to the case of the GaAs cell (section 4); and the layer thickness determination using spectral reflectivity (section 5).

2 FLUENCE AND DAMAGE CALCULATIONS

2.1 Fluence calculation

10 MeV proton energy is the standard energy used to simulate a space irradiation. The selected fluence represents the fluence received during a space mission in a Low Earth Orbit (LEO) during 8 years and it was determined using the method previously developed at DES [1]. This method considers the equivalence between space proton spectrum and the 10 MeV monoenergetic proton fluence based on the primary knock-on atoms (PKA) obtained using the TRIM (transport of ions in matter) software [2] for a simplified semiconductor structure representative of each sample. The details for the application of this method are published elsewhere [1, 3]. The spatial damage was simulated using a total spatial dose of 1.23×10^{12} proton.cm^{-2} calculated for III-V devices using the SPENVIS facility (see ref. [4]). The resulting fluence calculations for all devices are summarized in Table I.

Table I: Fluence calculations for the irradiated devices

Sample	Fluence (10^{11} p.cm^{-2})
InGaP/GaAs/Ge cell	3.7 ± 0.7
InGaP cell	4.0 ± 0.7
GaAs cell	3.8 ± 0.5
Ge cell	3.6 ± 0.5

2.2 Damage estimation

To estimate the irradiation damage on the different devices we studied the integral collisions spectra in depth (n_i) for transferred energies, E_{PKA}, higher than 10 eV, 100 eV and 1,000 eV. The spectra are obtained through simulations using the TRIM code. The presence of interfaces in the multilayer semiconductor structure generates artifacts due to discretization when the TRIM fast mode is used. To solve this problem, the step-by-step option of the code should be used. The improvement of this method is based on the segmentation of the spatial window at each molecular layer. Thus, the step-by-step method was applied to the first thin device layers and the fast method was applied to the substrate, optimizing the calculation time for a complete device study. For the

triple junction InGaP/GaAs/Ge solar cell step-by-step simulations with 10,000 protons were performed. The simulation in the substrate was studied afterwards using the fast method with 250,000 protons.

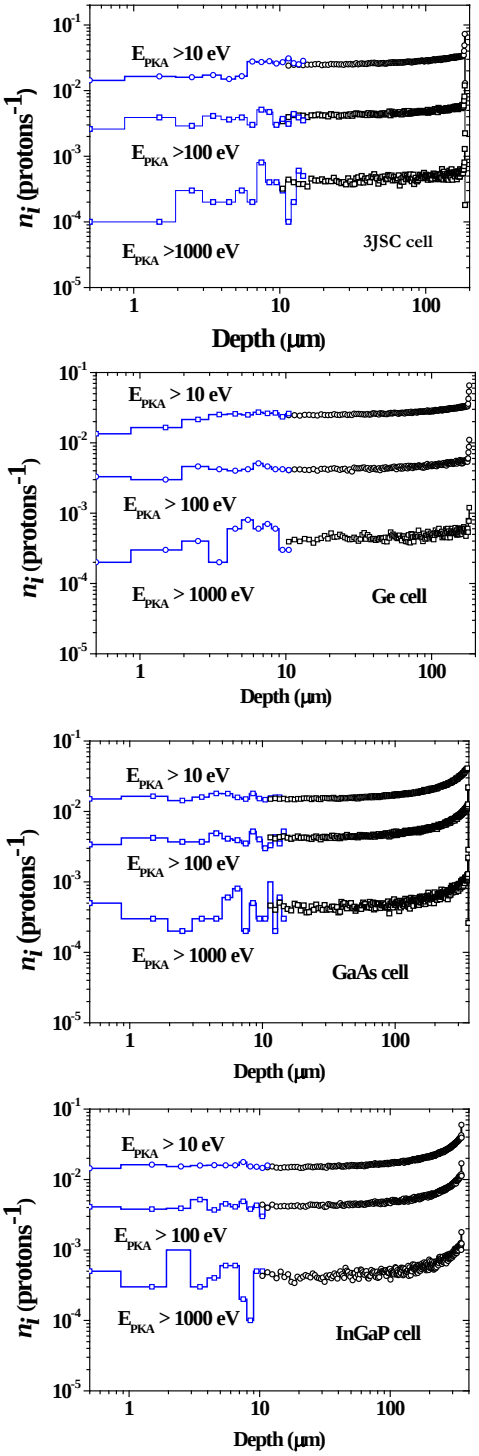

Figure 1. Collision spectra for all cells at PKA energies higher than 10, 100, and 1,000 eV, calculated using TRIM.

Figure 1 depicts the number of collisions as a function of depth for all four cells: 3JSC and Ge cells (Ge substrate); and GaAs and InGaP cells (GaAs substrate). The collisions are practically constant throughout the entire sample for all cases. At high depths, as the particles loose energy, a slight increment of the number of collisions is observed for GaAs and InGaP cells at the substrate level. An increased damage for the GaAs substrate is due to the higher thickness (350 µm) respect to the Ge substrate (180 µm) used in the 3JSC and Ge devices.

The statistical enhancement for lower energy transferred threshold smoothes the curve. For the Ge and 3JSC cells, a discontinuity in n_i appears at depths of 2 and ~ 6-7 µm, respectively, even at low energies (E_{PKA} > 10 eV) due to the change of material density. On the contrary for both cells grown onto GaAs wafer (GaAs and InGaP cells), there is no observable discontinuity at the front substrate surface.

3 EXPERIMENTAL RESULTS

3.1 Experimental setup

The 10 MeV beam distribution was determined by the current collected by 9 Faraday cups measured with a Keithley 6517 electrometer. All experiments were performed under vacuum using a specially developed chamber coupled to one line of the TANDAR accelerator (for more details see ref. [3]).

In order to monitor the degradation of the devices during irradiation, the beam was stopped at different fluences to measure the I-V curve. For instance, three doses were considered for the InGaP cell and five for the triple junction cell, GaAs cells and Ge diode. Instead, the GaAs/InGaP/Ge unprocessed wafer and the Ge (100) substrate received the total dose at once. Table II presents, as an example, the fluences actually received by the Triple Junction cell and the GaAs cell.

Table II: Accumulated fluences received by Triple Junction and GaAs cells

Fluence	GaAs (10^{10} x p.cm^{-2})	3JSC (10^{10} x p.cm^{-2})
1	0.27 ± 0.02	0.11 ± 0.09
2	1.0 ± 0.1	0.77 ± 0.26
3	5.8 ± 0.3	5.3 ± 1.5
4	15 ± 10^1	15 ± 2
5	51 ± 1	43± 2

All solar cells (3JSC, InGaP, and GaAs cells) were measured in situ before and after irradiation using a Sciencetech 1kW AM0 solar simulator coupled to the irradiation chamber through a borosilicate window and a SMU (source measure unit) Keithley 2602A in a four wire configuration. All I-V curves are presented under standard conditions (1 sun AM0, 28ºC) after temperature and irradiance correction.

3.2 In-situ illuminated I-V measurements

For the 3JSC and InGaP cells, degradation of the electrical parameters during irradiation was found negligible, but this is not the case for the GaAs cell. Figure 2 shows the results obtained for the GaAs cell, where a remarkable degradation of the cell efficiency is observed. Figure 3 depicts the evolution of J_{SC} and V_{OC} with the fluence normalized to the value previous to the irradiation. The main effect is observed on the decay of the $J_{SC,}$ which decreases almost 50% after the total irradiation whereas the *Voc* is only reduced by 5%.

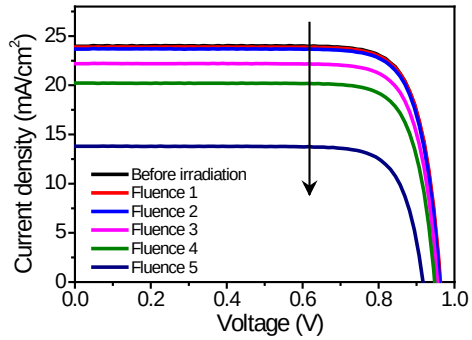

Figure 2: In-situ I-V curves measured under illumination for the GaAs cell at different irradiation fluences and corrected to standard conditions. The arrow represents the direction of increasing irradiation.

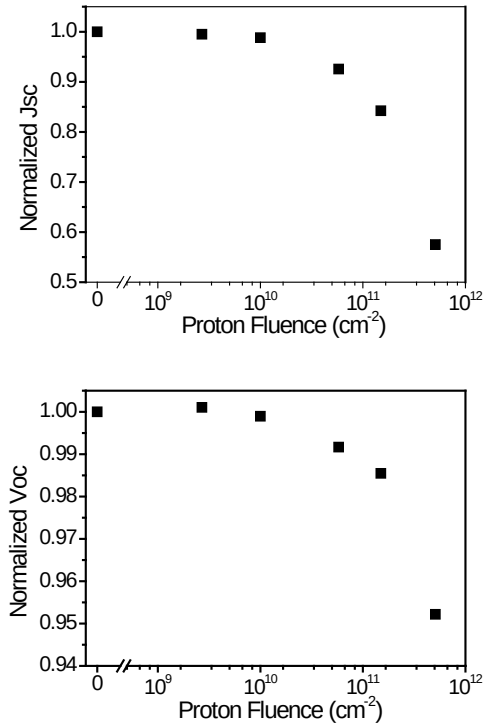

Figure 3: Electrical parameters (J_{SC} and V_{OC}) normalized to the value previous to irradiation versus fluence for the GaAs cell from Fig. 2.

Remarkably, as stated before, the 3JSC shows no appreciable degradation whatsoever. The lack of degradation for the 3JSC is unexpected for a couple of reasons. First, if the GaAs cell shows degradation when grown as a single junction, one can assume similar effects in the middle GaAs subcell of the 3JSC. Because the top InGaP and middle GaAs subcells are grown to have similar photocurrents, if degradation occurs, the middle cell would now limit the current, therefore impacting in the overall behavior of the 3JSC upon irradiation exposure. However, this was not observed as described above.

There is wide experimental evidence that GaAs cells show higher sensitivity to irradiation than InGaP or 3JSC InGaP/GaAs/Ge cells (see for instance ref. [5]). In this sense, our results are in agreement with previous observations. There is still much to understand about the degradation mechanisms that govern the GaAs cells damage and why the 3JSC performance is not affected by that. Numerical simulations of the devices presented in a section 4 below will shed some light into this issue.

3.2 In-situ dark I-V measurements

Dark curves corresponding to single junction devices were fitted using the two diode model:

$$I = I_{01}\left[\exp\left(\frac{V - IR_S}{m_1 kT/q}\right) - 1\right] + I_{02}\left[\exp\left(\frac{V - IR_S}{m_2 kT/q}\right) - 1\right] + \frac{V - IR_S}{R_P} \quad (1)$$

where I_{01} and I_{02} are the diode saturation currents, m_1 and m_2 are the ideality factors, R_S and R_P are the series and parallel resistances respectively, k is the Boltzmann's constant, T is the junction temperature, and q is the electronic charge. Fit results obtained for the GaAs and InGaP cells are summarized in Table III.

Table III: Parameters associated with the I-V dark curves fitting for the GaAs and InGaP cells.

GaAs cell				
Step	R_S [Ω]	m_1	I_{01} [A]	I_{02} [A]
0	0.055	1.40	4.6e-16	2.6e-12
1	0.059	1.34	1.1e-16	3.1e-12
2	0.061	1.33	9.4e-17	3.2e-12
3	0.072	1.33	9.9e-17	3.4e-12
4	0.079	1.32	1.2e-16	3.5e-12
5	0.092	1.32	1.9e-16	4.4e-12
InGaP cell				
Step	R_S [Ω]	m_1	I_{01} [A]	I_{02} [A]
0	0.153	1.47	4.5e-20	3.4e-8
3	0.161	1.53	2.6e-19	3.5e-8
4	0.272	1.62	2.5e-18	3.5e-8
5	0.332	1.62	3.1e-18	3.5e-8

The cell damage for the GaAs device reflected in the illuminated curves (Figure 2) is also evident in the corresponding dark curves, while for the cases of 3JSC and Ge diode there are virtually no observed changes. For the GaAs solar cell, parameters R_S and I_{02} increase with the fluence, while m_1 decreases and I_{01} remains basically constant. The increment of I_{02} indicates a higher influence of the non-radiative recombination processes at the perimeter and/or the space charge region [6]. For the InGaP cell the parameters R_S, I_{01} and m_1 increase with the fluence, while I_{02} remains almost constant. This behavior reflects the increase in defect densities in the quasi-neutral regions. However, these effects are not important enough to be reflected on the cell electrical parameters under illumination, as described in the previous section.

4 DEVICE NUMERICAL SIMULATION

Device simulation gives a physical insight in the internal processes occurring in electronic devices. We have previous experience in the application of the D-AMPS-1D [7-9] to III-V based solar cells [10-12]. In this work, we used the defect-pool model available in D-AMPS-1D [13] to represent the defect generation into the devices due to irradiation. A typical defect cross section of $1x10^{-15}cm^2$ was considered, and defect density for a

monoenergetic defect in the gap was tuned to fit experimental results. With this simple model we fit the experimental J_{SC} for the different accumulated fluences received by the device.

The first step was to fit the J_{SC} of the GaAs cell previous to irradiation. This defines an 'intrinsic' defect concentration. Both experimental J_{SC} and V_{OC} were successfully reproduced, as in our previous work with this type of devices [10]. Once the initial defect density was determined, this density was increased in order to match J_{SC} experimental values for each irradiation fluence. The simulated values, presented in Fig. 4, are in good agreement with the experimental J_{SC} with differences that do not exceed 1.3%. In a second step, the 3JSC GaAs middle subcell was simulated considering the optical filtered AM0 spectrum using the procedure described in [11] and the same defects densities found previously for the homojunction GaAs cell. The spectral content of the incident illumination is calculated using the Optical code for the entire 3JSC structure, so that all optical interference phenomena are considered.

Figure 4 presents the simulated J_{SC} values obtained for both the GaAs homojunction and the middle GaAs cell in the 3JSC. Strikingly, the GaAs middle subcell does not present an appreciable degradation of the J_{SC} that remains almost constant for all irradiation fluences. On the contrary, the GaAs homojunction shows a marked reduction of the J_{SC} upon irradiation as expected from the experimental illuminated I-V curves. These simulation results support the experimental evidence obtained from the illuminated I-V curves for the irradiated 3JSC that indicated no appreciable damage. At this point it is hard to speculate on the origins of the dissimilar behaviors for both cells, however, we must note that the device thicknesses differ for both cells and also that the spectral content is modified due to the presence of the top cell. Further detailed simulations need to be performed in order to understand this behavior.

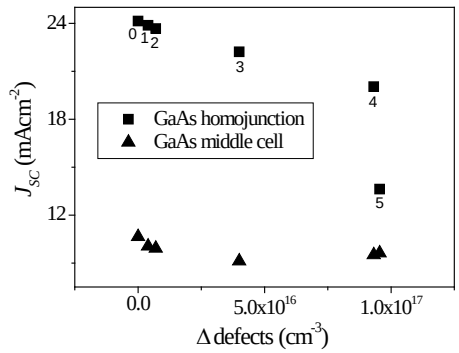

Figure 4. Simulated J_{SC} for the GaAs homojunction and 3JSC GaAs subcell versus defect density referred to the initial condition before irradiation (Δ defects). Numbers refer to the steps in the irradiation experiment.

5 MATERIALS CHARACTERIZATION

Materials characterization was performed onto a GaAs/InGaP/Ge structure and an unprocessed Ge wafer.

Spectral reflectivity was measured on the samples using a GBC spectrophotometer with an integrating sphere. Later, the reflectivity was theoretically simulated using the code Optical [14]. Refractive indexes were obtained from literature (refs. [15-17]). Theoretical fitting using Optical allows determining layer thicknesses by minimizing the difference between experimental and theoretical curves, Table IV and Figure 5. The good fitting results and the small differences in thicknesses show a quite good reproducibility of the epitaxy process.

Table IV: Nominal thicknesses and calculated thicknesses from reflectivity for the GaAs/InGaP/Ge sample.

Thickness	GaAs (nm)	InGaP (nm)
Intended	950	350
Fitting with Optical	975	380

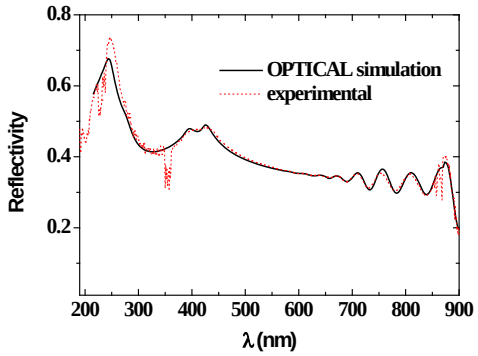

Figure 5. Spectral reflectivity of the GaAs/InGaP/Ge structure and theoretical simulation using Optical.

μ-Raman measurements were done with a LabRam XY spectrometer, focusing a 514.9 nm line of an Ar^+ laser onto the sample by the microscope objective, which also collects the scattered light, thus conforming a nearly backscattering geometry. With three different microscope objectives we obtained a diameter laser beam between 1 and 100 μm at the focal plane. Since the Raman spectrum is sensitive to the crystallographic order, one can expect a dependency of the position or shape of the phonon peaks on the defects structure. In particular, the InGaP structure presents two modes for lattice matched composition (InP-like or GaP-like), which additionally couple with the plasmon mode if the system is doped. This system is very sensitive to changes in the charge carrier concentration and to the atoms arrangement. Preliminary investigation of Raman spectra do not show any difference between irradiated and no-irradiated samples when exciting on the front and the back of the sample. This situation was verified for both samples studied, a Ge wafer and a Ge cell structure (GaAs/InGaP/Ge).

As a preliminary conclusion, Raman spectroscopy has not enough sensitivity to reveal the damage produced by the irradiation. As showed in Figure 1, in Ge substrates the damage is quite uniform because high energy ions pass through the sample and are not stopped at any point inside the sample. The produced damage is then probably not so substantial to produce observable changes in the crystallographic structure.

6 CONCLUSIONS

A 10 MeV proton irradiation experiment was performed on III-V semiconductor materials and solar cells. The irradiation fluences were calculated to emulate the situation of 8 years in a LEO orbit using a model based on PKA spectrum for each structure. Simulations

using the TRIM code in the step-by-step mode allowed having a picture of the damage distribution in all tested devices. This damage is quite uniform, with some differences if the substrate is GaAs or Ge.

The analysis of the in-situ dark I-V curves depicted tendencies of the behavior under irradiation for the GaAs and InGaP cells. Electrical parameters taken from in-situ illuminated I-V curves showed no changes for 3JSC and InGaP cells, while GaAs cell exhibited a visible degradation. The apparent inconsistency between 3JSC and GaAs cell behavior under irradiation was confirmed through the results obtained by device numerical simulations, although the reasons of the irradiation insensitivity of the 3JSC GaAs middle cell are still not clear.

7 ACKNOWLEDGEMENTS

This work was funded by CNEA, the grants PIP2009-2011 Nº 02318 (CONICET) and PICT2007 Nº 01143 (ANPCyT), and the bilateral collaboration MINCyT-MICINN 2012-2013 (Argentina-Spain) Nº ES/11/04 "Fabrication, characterization, simulation and test on solar cells based on III-V semiconductors". The authors acknowledge to M.E. Reinoso for her help in Raman measurements.

8 REFERENCES

[1] M. Alurralde, Method using the primary knock-on atom spectrum to characterize electrical degradation of monocrystalline silicon solar cells by space protons, Journal of Applied Physics 95 (2004) 3391.

[2] J. F. Ziegler, http://www.research.ibm.com/ionbeams, 2003.

[3] A. Filevich, C.J. Bruno, J. Fernández Vázquez, M. Alurralde, I. Prario, M.J.L. Tamasi, M.G. Martínez Bogado, J.C. Plá, J. Durán, J. Schuff, A. Burlon, P. Stoliar, D. Minsky, A.J. Kreiner, R. Mayer, A compact portable set up for in situ solar cells degradation studies, IEEE Transactions on Nuclear Science 50 (2003) 2380.

[4] R.J. Walters, J.H. Wamer, G.P. Summers, S.R. Messenger, J.R. Lorentzen, Radiation response mechanisms in multijunction III-V space solar cells, Proceedings 31st IEEE Photovoltaic Specialists Conference, (2005) 542.

[5] M. Alurralde et al., Development of solar arrays for Argentine satellite missions, Aerospace Science and Technology 26 (2012) 38.

[6] P. Espinet, C. Algora, J. González, N. Núñez, M. Vázquez et al., Degradation mechanism analysis in temperature stress tests on III-V ultra-high concentrator solar cells using a 3D distributed model, Microelectronics Reliability 50 (2010) 1875.

[7] M. Vukadinovik, F. Smole, M. Topic, R.E.I. Schropp, F.A. Rubinelli, J. Appl. Phys. 96 (2004) 7289.

[8] P.J. McElheny, J.K. Arch, H.S. Lin, S.J. Fonash, J. Appl. Phys. 64 (1988) 1254.

[9] F. Rubinelli, S.J. Fonash, J.K. Arch, in: Proceedings of the 6th International Photovoltaic Science and Engineering Conference, NewDelhi, India, 1992, p. 811

[10] J. Plá, M. Barrera, F. Rubinelli, The influence of the InGaP window layer on the optical and electrical performance of GaAs solar cells, Semiconductor Science and Technology 22 (2007) 1122.

[11] M. Barrera, J. García, H. Socolovsky, F. Rubinelli, E. Godfrin, J. Plá, Activities on simulation and characterization of multijunction solar cells for space applications in Argentina, Proceedings 23rd European Photovoltaic Solar Energy, (2008) 781.

[12] M. Barrera, F. Rubinelli, I. Rey-Stolle, J. Plá, Numerical simulation of Ge solar cells using D-AMPS-1D code, Physica B 407 (2012) 3282.

[13] E. Klimovsky, A. Sturiale, F.A. Rubinelli, Characteristic curves of hydrogenated amorphous silicon based solar cells modeled with the defect pool model, Thin Solid Films 515 (2007) 4826.

[14] E. Centurioni, Generalized matrix method for calculation of internal light energy flux in mixed coherent and incoherent multilayer, Applied Optics 44 (2005) 7532.

[15] R.F. Potter, Germanium, in Handbook of optical constants of solids, edited by E. Palik, Academic Press, Vol. 1 (1985).

[16] E. Palik, Gallium arsenide, in Handbook of optical constants of solids, edited by E. Palik, Academic Press, Vol. 1 (1985).

[17] M. Schubert, V. Gottschalch, C.M. Herzinger, H. Yao, P.G. Snyder, J.A. Woollam, Optical constants of $Ga_xIn_{1-x}P$ lattice matched to GaAs, Journal of Applied Physics 77 (1995) 3416.